International Journal of Geo-Information

MDPI

Article

Mapping Spatiotemporal Patterns and Multi-Perspective Analysis of the Surface Urban Heat Islands across 32 Major Cities in China

Juan Wang [1,2], Bin Meng [1,*], Dongjie Fu [2], Tao Pei [1,2] and Chengdong Xu [2]

[1] College of Applied Arts and Sciences, Beijing Union University, Beijing 100191, China; wangjuan@buu.edu.cn (J.W.); peit@lreis.ac.cn (T.P.)

[2] State Key Laboratory of Resources and Environmental Information System, Institute of Geographic Sciences and Natural Resources Research, Chinese Academy of Sciences, Beijing 100101, China; fudj@lreis.ac.cn (D.F.); xucd@lreis.ac.cn (C.X.)

* Correspondence: mengbin@buu.edu.cn; Tel.: +86-010-6200-4545

Received: 29 March 2018; Accepted: 27 May 2018; Published: 30 May 2018

Abstract: As urban thermal environments are being caused by global climatic changes and urbanization is not uniform on diurnal, seasonal, or annual scales, the spatiotemporal patterns of surface urban heat islands (SUHI) similarly vary between cities across regions. This research assessed the spatiotemporal variations in SUHI intensities (SUHII), and then revealed their spatiotemporal patterns and relationships that existed within 32 major cities in China using spatialization technologies, such as the self-organizing map (SOM) method and statistical methods. Results showed that the spatial patterns of the SUHII patterns in China were significantly affected by the climatic types, whereas human heat discharge also disturbed the patterns to a certain extent. Specifically, the daytime SUHIIs in China had much higher seasonal variations in North China than in South China. The nighttime SUHIIs were much weaker and more stable than the daytime SUHIIs, and had far more obvious spatial patterns with much higher values in North China than in South China. As for the temporal regimes, the temporal variation in the SUHIIs in one city was more related to the development of the urbanization. To be specific, not all cities were experiencing increasingly worse urban thermal environments with urbanization as reported by previous studies. This research not only proposes a spatiotemporal framework to study the SUHIIs patterns and their relationships, but also provides an in-depth and comprehensive understanding of SUHIIs in China.

Keywords: surface urban heat island; spatiotemporal patterns; climatic zones; urbanization; China

1. Introduction

Rapid urbanization has resulted in faster urban climate change compared with global changes, especially in developing countries such as China [1]. One of the environmental consequences of urbanization is the urban heat island (UHI) effect, whereby urban centers experience higher temperatures than surrounding rural areas [2]. Although UHIs only cover a tiny fraction of the global surface area and is just a small-scale phenomenon [3], they can, nonetheless, directly affect the lives of local people in cities, indicated by the high demand for air conditioning energy, high heat-related disease and air pollution [4–6]. Therefore, understanding the UHI phenomenon and its patterns are of great importance to help the decision-makers take mitigation measures when developing and executing rational land use policies.

Different types of UHIs have been defined according to the different urban layers, including the surface urban heat island (SUHI) based on the land surface temperature (LST) of the urban

surface layer, and the atmospheric urban heat island (AUHI) based on the air temperature of the urban boundary or canopy layer [7]. Although these two kinds of UHIs have different underlying meanings, they were related with each other and can both satisfactorily explain the UHI effect [2]. The station-based temperatures were discretely observed and cannot reveal the spatial heterogeneity in urban environments [8–10]. LST derived from thermal infrared remote sensing (TIR) has been widely used in SUHI studies due to its large-area coverage and relatively high temporal frequency advantages. LST is especially useful for understanding the spatio-temporal variations in SUHI [7,11]. In these SUHI studies, the SUHI intensity (SUHII) is a commonly used indicator when quantifying the SUHI magnitude, which was defined as the LST differences between the urban and surrounding rural areas (Section 2.2.1). Generally, the SUHI studies based on TIR can be categorized into two groups: studies for one single city at the micro-scale and studies for multiple cities at the meso-scale. At the micro-scale, considerable progress in the intra-city SUHI studies has occurred based on medium high spatial resolution (e.g., Landsat TM/ETM+), which usually focuses on the spatial patterns of land surface temperature (LST) and its relationship with the urban surface characteristics as indicated by land use and land cover types, vegetation indexes, and urban landscapes or structures [3,7,11–19]. Although these categories of research demonstrated the detailed spatial heterogeneity of the SUHII, the trade-off between the spatial and temporal resolution complicated the conducting of continuous long-term series monitoring and the comparative understanding of SUHII between cities in the regions. With the accumulation of meteorological satellite datasets with high temporal resolution, such as Moderate Resolution Imaging Spectroradiometer (MODIS), regional or global SUHI studies have attracted considerable attention, as these categories of SUHI studies provide a comprehensive and comparative understanding 0f the SUHIs [20]. A series of SUHI studies of tropical mega-cities, populous cities in the United States, European cities, and even cities worldwide, have been reported [21–25]. These studies demonstrated that the surrounding ecological conditions of one urban area may play an important role in the variation of SUHI on the meso-scale, and the background and local climate zones also greatly affected the SUHI [26]. Among the SUHI studies on the regional scale, those conducted in China were prominent, as China has experienced rapid urbanization and the SUHIs have been recorded not only in mega cities such as Beijing [27], Shanghai [28] Shenzhen [29], and Guangzhou [30], but also in other smaller cities such as Kunming [31], Guizhou [32], and Baotou [33]. Meanwhile, China includes many climatic types, which made it particularly practical and academically interesting to investigate the SUHII in China on the meso-scale. Zhou et al. [34–36] and Yao et al. [37] determined the SUHIs on the meso-scale for 32 major cities in China and highlighted the spatial patterns, drivers, and the effect of urbanization levels on the SUHII based on statistical approaches using time-series remote sensing images [34–37]. This series of works considerably progressed the understanding of the SUHI in China. However, these works only focused on subjectively demonstrating the patterns, but did not automatically or objectively reveal the internal spatial and temporal similarities and differences between regions. Therefore, further studies are needed to present the regional regularity to fill this research gap.

The self-organizing map (SOM) method is one kind of unsupervised neural network to automatic cluster and reduce dimensionality [38]. As the weights of the neurons in the output layer in a trained SOM are dependent on the number of neurons, a low dimensional model with high-dimensional input space and a low-dimensional representation of high-dimensional vectors can be obtained after mapping onto the trained SOM, which makes it particularly suited for handling voluminous and high-dimensional datasets [39]. Additionally, as the SOM can reflect the local projection of the principal components of the input data, SOM can be regarded as a manifold to the data space that is often useful in explaining observed patterns and understanding complex relationships within the input data [40]. These characteristics qualify SOM as a powerful geographic data analysis tool, enabling its use with geographically referenced environmental data [41]. Therefore, we used the SOM method to visualize spatiotemporal clustering and the inner regularities of the SUHIIs in China. By choosing 32 major cities in China for our study, this research aimed to provide spatiotemporal mapping and

multi-perspective understanding of the SUHIs in China and then address the following questions: (1) How did the background climatic types accompanied by intensive human activities affect the spatiotemporal patterns of the SUHI? (2) Were the SUHIIs in major cities in China worsening or improving during the past decades? Structurally, the spatiotemporal variations in SUHII across major Chinese cities are first presented and the differences between climatic zones are highlighted. Following this, the clustering and the spatiotemporal patterns of the SUHIIs in China are automatically recognized and visualized. The potential factors are also presented to explain those recognized patterns.

2. Methodology

2.1. Study Area

China is located in the eastern part of the Asian continent west of the Pacific, and has experienced rapid urbanization since initiating its reform and opening up policy in 1978. Increasing urban land cover and population have caused a series of urban environmental effects in China, among which urban heat islands are the most common. China has abundant climate types, including five climatic zones from north to south, including Zone 1 (severe cold region); 2 (cold region); 3 (hot summer; cold winter region); 4 (temperate region); and 5 (hot summer, warm winter region) (Figure 1). This classification system is based on the different seasonal characteristics and is closely correlated with people's lives and the building design standard in China [42], both of which have obvious effects on the urban thermal environment and are thus suitable for SUHII studies. Additionally, the differences allow the division of varying geographic environments and energy use between North and South China divided by the Qinling-Huaihe Line [43], which is also along these climatic zones. We selected 32 provincial capitals and municipalities in China as the study area (Figure 1). The location of each city (latitude and longitude) was derived from the geographical database from the GeoNames geographical database (http://www.geonames.org/) and then visualized in projected coordinates (Albers conical equal area), which is commonly used in China. The summarized information for the selected cities is listed in Table 1.

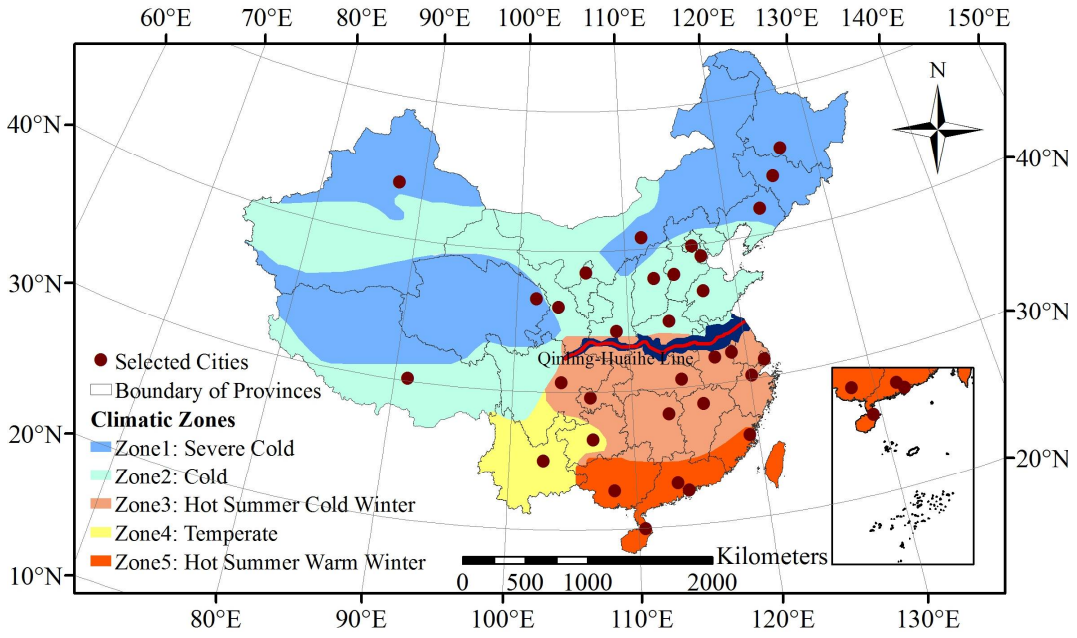

Figure 1. The study area and the distribution of selected cities in this research.

Table 1. Summarized information for selected cities examined in this research.

City	Lat.	Lon.	Urban Area (2010; km^2)	Rural Area (2010; km^2)	Pop. in 2010 (Unit: 10,000, People)	Annual Change Rate (CR) of Pop. (2003–2013)
Beijing	39.91	116.40	1902	5146	1258	15.99
Chengdu	30.67	104.07	582	6618	1149.07	13.96
Fuzhou	26.06	119.31	467	1371	645.9	5.40
Guangzhou	23.12	113.25	1069	1923	806.14	10.71
Guiyang	26.58	106.72	162	1504	373.16	3.63
Harbin	45.75	126.65	727	26,919	992.02	3.46
Haikou	19.96	110.52	111	596	160.44	2.40
Hangzhou	30.26	120.17	337	1957	689.12	6.15
Hefei	31.86	117.28	174	6256	493.42	28.63
Hohhot	40.81	111.65	187	1670	229.56	2.30
Jinan	36.67	117.00	279	7215	604.08	2.34
Kunming	25.04	102.72	838	3958	536.31	5.08
Laksa	30.17	91.13	31	176	48.46	1.49
Lanzhou	36.06	103.79	447	181	323.54	3.94
Nanchang	28.68	115.88	166	4988	502.25	5.61
Nanjing	32.06	118.78	230	4860	632.42	6.90
Nanning	22.82	108.32	427	2083	707.37	8.31
Shanghai	31.22	121.46	1503	4160	1412	9.44
Shzhen	22.55	114.07	680	293	259.87	15.37
Shenyang	41.79	123.43	668	11,343	719.6	3.86
Shijiangzhuang	38.04	114.48	986	10,154	989.16	10.42
Taiyuan	37.87	112.56	310	1866	365.5	4.12
Tianjin	39.14	117.18	970	7704	985	7.49
Urumqi	43.80	87.58	329	280	243.03	8.84
Wuhan	30.58	114.27	490	5572	836.73	4.26
Xian	34.26	108.93	447	4529	782.73	8.75
Xining	36.62	101.77	333	487	196.01	3.87
Yinchaun	38.47	106.30	118	1505	158.8	3.78
Changchun	43.88	125.32	586	18,245	758.89	4.04
Changsha	28.20	112.97	252	4055	650.12	6.01
Zhengzhou	34.76	113.65	552	6437	744.62	36.52
Chongqing	29.56	106.55	539	16,544	3303	24.26

2.2. Datasets and Methodology

2.2.1. Surface Urban Heat Island Intensity Calculation

As one main indicator of the SUHI, the (SUHII) is defined as the difference in the land surface temperature (LST) between the urban area and its surrounding rural area. SUHII can be calculated by the following formula:

$$SUHII = T_{urban} - T_{rurual} \quad (1)$$

where, T_{urban} is the spatially averaged LST over the urban area and T_{rural} is the spatially averaged LST over the rural area. Therefore, to calculate the SUHII, two key steps are needed: LST derivation and urban/rural area extraction.

LST Derivation

Version 5 of MYD11A2 products were obtained to derive the long-term LST series from the National Aeronautics and Space Administration (NASA) EarthData Search (https://search.earthdata.nasa.gov/search). This dataset includes both the daytime (local time ~01:30 p.m.) and nighttime (local time ~01:30 a.m.) temperature from 2003 to 2013, with a spatial resolution of 1 km and an 8-day interval temporal resolution. The dataset was improved by correcting noise due to cloud contamination, topographic differences, and zenith angle changes. The dataset had high accuracy with low root mean squares differences based on the surface emissivity evaluations [44]. The invalid data were eliminated using the quality assurance (QA) flags included in the product. In this research, only those pixels of good quality (Bits 0-1 are 00) were selected by reading the flags stored in an 8-bit unsigned integer. The seasonal averaged method was also employed to reduce the noise effect. Finally,

seasonal averaged LST datasets in both daytime and nighttime during the study period were derived to calculate the SUHIIs.

Urban and Rural Area Extraction

Usually, relatively clear definition and approved extraction methods are available for urban areas, which refer to the built-up areas in a city. The urban area can be determined based on the nighttime lights or the land use and land cover (LULC) maps. For rural areas, at present there is no recognized method for the SUHII calculation, but it is commonly subjectively derived based on the buffering zone of the urban area [24,34,45]. Additionally, the LULC types surrounding urban areas can also affect the temperature gradient between the urban and rural zones if the buffering zones are directly used to extract the rural area [46]. Urban and rural areas have been clearly defined in urban geography research. Urban areas refer to the center of the city and the surrounding continuous built-up area, whereas rural areas refer to those areas other than urban areas within the administrative area [47]. Based on this definition and considering the effects of the elevation and water on the SUHII calculation, the urban/built-up area and the cropland area within the administrative area were considered as the urban and rural areas in this research, respectively.

For this purpose, the annual LULC products (MCD12Q1) from 2003 to 2013 were downloaded from the NASA EarthData Search (https://search.earthdata.nasa.gov/search). The LULC maps provide a land-cover type assessment and quality-control information. In this research, only those pixels with good quality were used, and the International Geosphere-Biosphere Programme (IGBP) global vegetation classification scheme layer was used, which included 16 land cover types. Further detailed information in the report of Friedl et al. [48]. In this research, after pre-processing (mosaic, re-project, and clip) using MODIS Reprojection Tool (MRT) software, the administrative boundary of each city was then overlaid with the LULC maps year by year. The urban/built-up area type was extracted as the urban area and the cropland type was extracted as the rural area for each year. That is, there were 11 urban and rural areas for each city in the study area from 2003 to 2013. Using Beijing as an example, its 2010 urban and rural areas are shown in Figure 2. Finally, the urban and rural areas in grid format were batch converted into vector format for further calculating the spatially averaged LST in the urban area (T_{urban}) and the LST in the rural area (T_{rural}). The remote sensing (RS) datasets used in this research are summarized in Table 2.

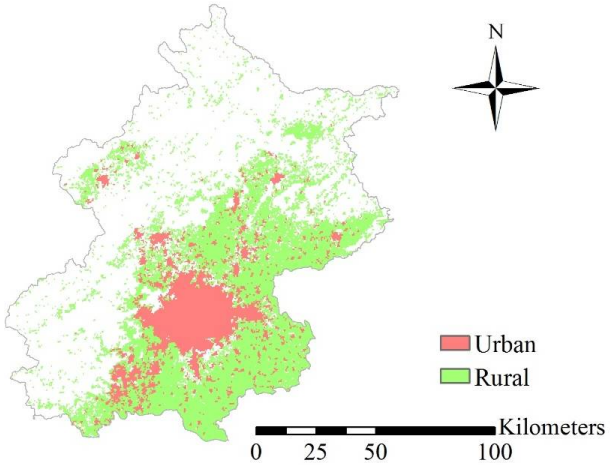

Figure 2. The urban and rural areas of Beijing City in 2010.

Table 2. The summarized details of remote sensing (RS) Datasets used in this research.

Name	Product	Pixel Size	Temporal Granularity	Timeframe	Source
MYD 11A2	Land surface temperature	1000 m	8-day	2003–2013	https://search.earthdata.nasa.gov/search
MCD 12Q1	Land cover	500 m	annually	2003–2013	https://search.earthdata.nasa.gov/search

SUHII Calculation

The SUHIIs were calculated as the difference in urban LST minus rural LST. Daytime and nighttime SUHII were calculated separately from Earth Observing System-Aqua-MODIS LST in the early afternoon (local time ~13:30 p.m.) and at night (local time ~01:30 a.m.), respectively. The seasonal and annual averaged daytime and nighttime SUHII were also calculated.

2.2.2. Spatiotemporal Mapping and Multi-Perspective Analysis of the SUHIIs

SOM Model

The SOM model is one of the unsupervised learning clustering methods, which is essentially a neural network with only an input layer, a hidden layer, and a target output. A node in the hidden layer represents a clustering that must be aggregated. The "competitive learning" method is used when training the network, and each input sample finds a matching node in the hidden layer, which is called the "winning neuron". The parameters of the activation node are updated using the stochastic gradient descent method. At the same time, the points adjacent to the activation node also appropriately update the parameters based on their distance from the activation node. Therefore, one of the features of SOM is that the nodes of the hidden layer are topological. Therefore, the SOM can discretize the input of any dimension to the discrete space of one or two dimensions. The nodes in the computation layer are fully connected to the Input layer nodes. Detailed information about the SOM algorithm can be found in the report of Kohonen) [49]. This research used SOM packages in R software for data processing and analysis.

Experiments in this Research

To provide a comprehensive and comparative mapping of the spatiotemporal patterns of the SUHIIs, both the seasonally averaged daytime and nighttime SUHIIs for selected cities are first presented. Then they were averaged over each climatic zone in China and analyzed comparatively using statistical methods.

As the high summer temperatures directly impact human comfort in Chinese cities, the spatiotemporal variations and clustering patterns in the daytime SUHIIs in summer during the study period are presented using the SOM method. As the input data, the original datasets were first organized into a matrix of 32 rows × 11 columns, which means that 32 cities were investigated, each with 11-year daytime SUHIIs in summer from 2003 to 2013. The target output was the clusters generated by the SOM. Before using the SOM method in this research, the SUHII values were normalized using three alternative methods, each of which could illuminate different relationships among the cities. In each case, normalization was based on scaling values in the range of 0 to 1, proportional to the minimum and maximum SUHII values.

(1) Globally Normalized. All SUHII values were normalized to 0–1 in a single step, based on the smallest and largest value ever observed for any city and any time period. Clusters among cities observed in the visualization, as expressed by the same colors, is thus largely reflective of differences in the SUHIIs.
(2) Column Normalized. Normalization occurred here in isolation for each time slice, based on minimum and maximum values for the respective slice. Assuming that the geographic distribution

of relative SUHII at different times was relatively constant, in that the relative ranking of cities does not change despite changes in absolute magnitudes, similar patterns of cities were expected to be close to what is produced by global normalization.

(3) Row Normalization. This is another form of normalization occurring within cities, that is, within rows of the input matrix. With the smallest and largest value ever observed for a particular city driving the normalization, this leads to the ability to more directly compare temporal SUHII signatures. For example, row normalization allows temporal alignment of local maxima and minima of different cities to be recognized despite differences in magnitude. Broad regional patterns affecting SUHII were expected to be highlighted using this approach, since regional causes may drive SUHII up or down in similar patterns.

The target output clusters generated by SOM was visualized in ARCGIS software. The cities in one cluster were labeled in the same color to demonstrate spatial patterns. To explain the above patterns derived from the SOM method, the spatial patterns in the annual averaged daytime SUHIISs during the study period are presented. The change rate was also computed using the least square method to test whether the SUHI worsened or improved with the development of urbanization. The formula for the change rate is as follows.

$$CR = \left(\overline{xy} - \overline{x} \cdot \overline{y}\right) / \left(\overline{x^2} - (\overline{x})^2\right) \quad (2)$$

where CR is the change rate; x is the independent variable, which refers here to the time and; y is the dependent variable, which refers here to the SUHII values. If the change rate was less than 0 in one city, the thermal environment was improving, otherwise, it was worsening.

The work flowchart in this research is summarized in Figure 3. First, the LST and LULC datasets were batch pre-processed in the MRT software. Then, the spatial overlaying analysis in ARCGIS software was used to calculate the SUHII combined with the geographical databases. The SOM method was programmed in the R software using R language. Finally, the SOM clustering results were visualized in ARCGIS.

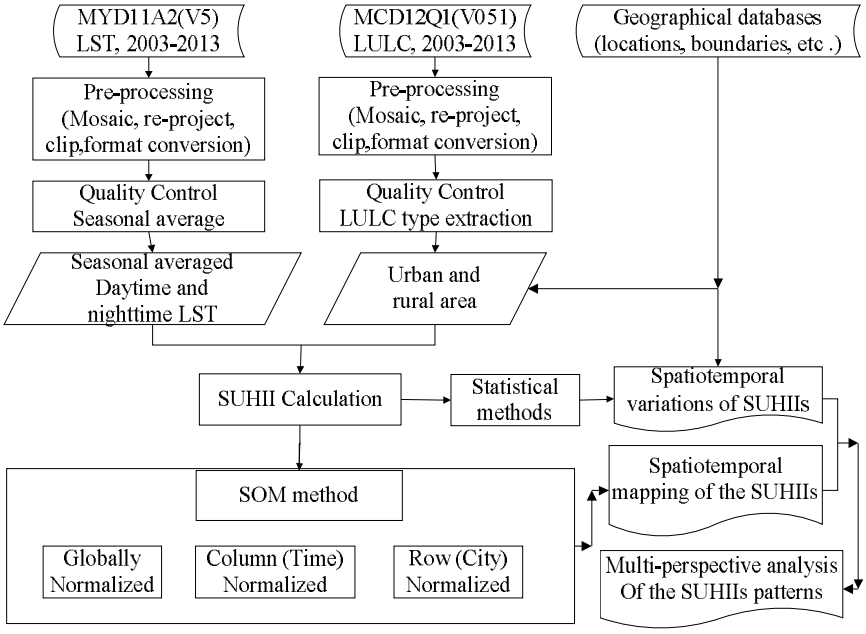

Figure 3. Flow chart in this research.

3. Results and Discussion

3.1. Spatiotemporal Variation of the SUHIIs

To provide a comparative understanding of the spatiotemporal variations in the SUHIIs in the study area, both the seasonal averaged daytime and nighttime SUHIIs values and their variances were calculated in each climate zone over four seasons. The results are shown in Figure 4. We found that both the daytime and nighttime SUHI had different intensities and seasonal variation between climate zones. Whereas nighttime SUHIIs were significantly more moderate than the daytime SUHIIs and more stable with smaller standard errors over the four seasons, daytime SUHIIs had more obvious seasonal variations in each climate zone. The strongest SUHIIs occurred in summer in all zones except in Zone 5, where the daytime SUHIIs in autumn had the largest value. This may due to the effect of the special climatic type in Zone 5, which was characterized by a hot summer and warm winter. The autumn was quite short and similar to summer. Therefore, the SUHII in autumn was unsurprisingly quite high in Zone 5, as the autumn (including September, October, and November in this research) was quite hot or even hotter in Zone 5. During the daytime, the lowest SUHIIs occurred in winter in all zones, with a value of less than 1 K in Zones 1, 4, and 5. Notably, the cities in Zones 2 and 3 had "urban cool islands" with negative SUHIIs in winter. Previous studies also found similar results for a few single cities such as Beijing [27]. This study further demonstrated that this is a universal phenomenon in Zone 2 in China. This may be due to the low thermal inertia of the bare and dry soil in rural areas and the high thermal inertia of the concrete material used in urban construction [50].

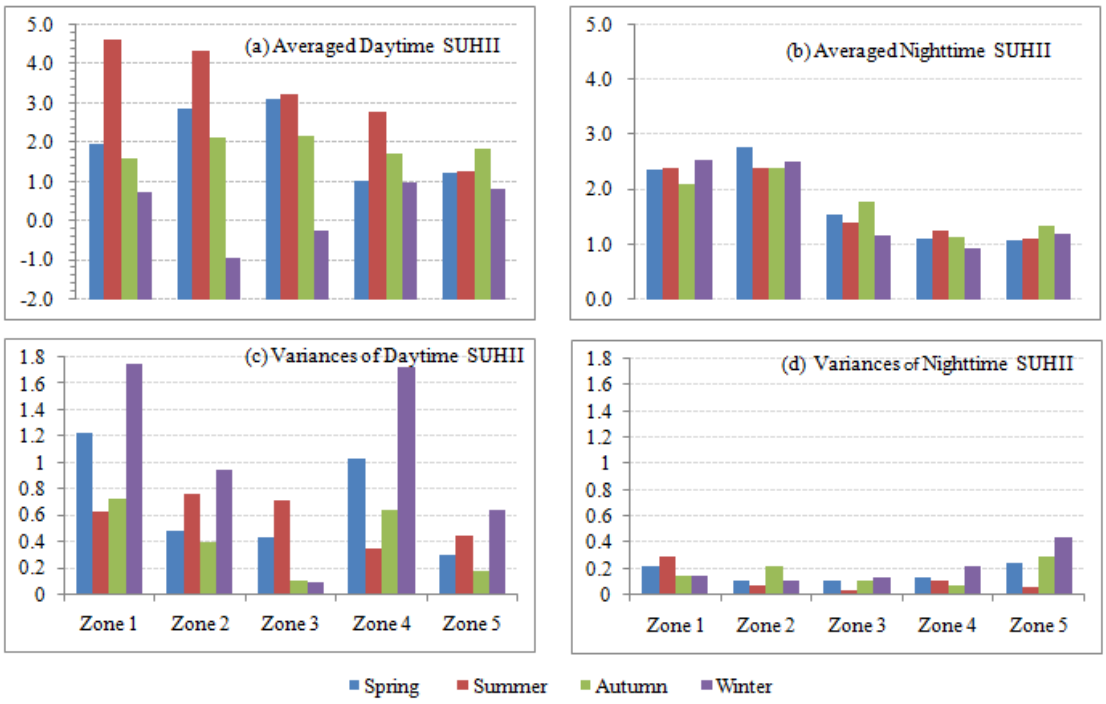

Figure 4. Seasonal averaged surface urban heat islands intensity (SUHII) values and their variances from 2003 to 2013 for different climate zones. Zone 1: severe cold region, Zone 2: cold region; Zone 3: hot summer cold winter region, Zone 4: temperate region, and Zone 5: hot summer warm winter region.

The seasonal variation in the nighttime SUHIIs was relatively smaller than the daytime SUHIIs, with about 2.5 K in Zones 1 and 2 about 1.5 K in Zones 3–5 over the four seasons. According to Oke [2], the nighttime urban thermal environment is mainly dominated by anthropogenic heat and radioactive cooling. Although the work generally focused on air temperature UHI, this was also helpful for

explaining SUHI, as land surface temperature was significantly correlated with air temperature [51]. Additionally, at the city scale, the population during the daytime was almost double that of the nighttime population, which may have increased anthropogenic heating magnitude with population density [52]. The temporal variability in anthropogenic heating may also affect the diurnal variation in the SUHI. These estimations explain why the nighttime SUHI was rather stable and reveal the relatively higher SUHIIs during winter.

Above all, the described diurnal and seasonal spatiotemporal variations in the SUHIIs suggest that daytime and nighttime SUHI had different mechanisms. The different physical processes for different climate types also form the different characteristics of the SUHIIs. We should consider the climatic types when studying the factors related to the spatial patterns of the SUHII.

3.2. *Spatiotemporal Mapping of the SUHIIs*

The results obtained using the SOM method using global, column, and row normalization are shown in Figure 5. As the SOM method outputs clusters labeled with numbers for each group of cities, the cities in the same cluster were labelled with the same color and then visualized in the GIS environment. Notably, all the three sub-graphs were completely independent with no coordination of color schemes. That is, cities with the same cluster were in red for the column normalized solution, but may also occur in purple for the row normalized solution. The main purpose of these visualizations was to observe multi-temporal regionalization of the SUHIIs across cities in different climatic zones.

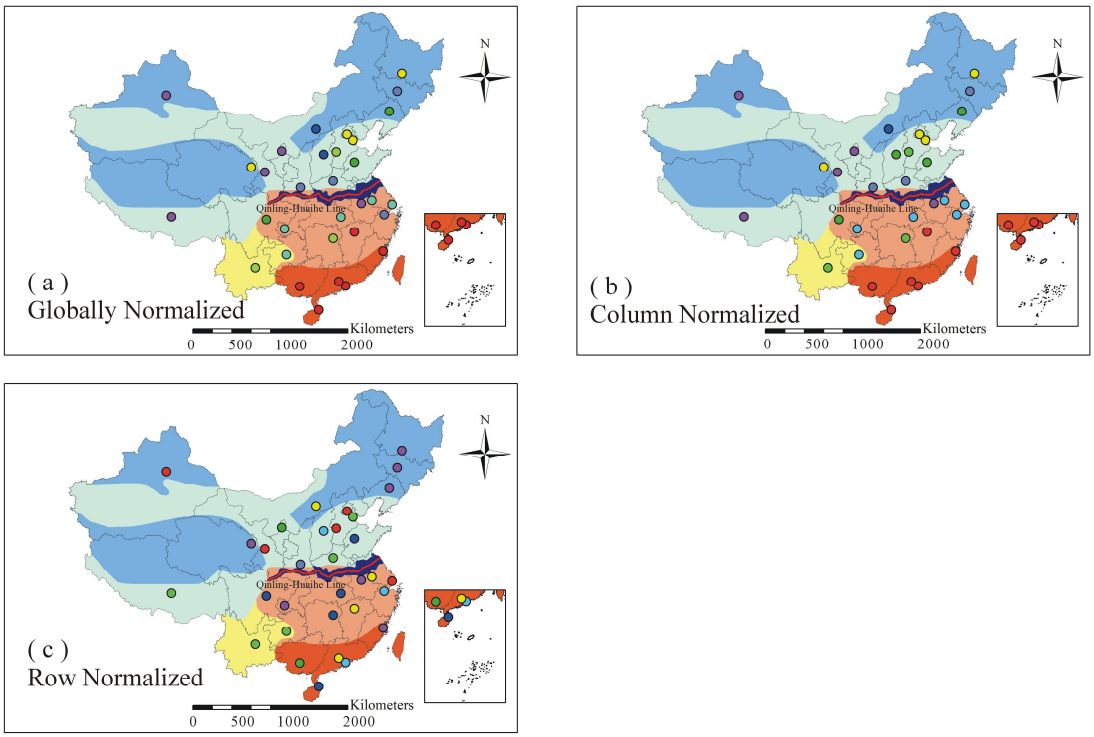

Figure 5. Self-organizing map (SOM) clustering results based on the SUHII calculated using the following normalization methods: (**a**) global; (**b**) column; and (**c**) row.

As expected, the column normalized and the globally normalized SOM method demonstrated very similar patterns, which are shown in Figure 4a,b, respectively, which can be explained by the mechanism of the SOM method. We have known that the column normalized way could emphasize and highlight the spatial (regional) effect. As the spatial distributions of the relative SUHII values between different years were relatively stable, the relative order of the cities remained unchanged despite changes occurring in the absolute magnitudes of the SUHIIs. Therefore, the city patterns using

the column normalized were expected to be similar to the patterns produced with global normalization. Regardless, using both normalization methods, the clustering spatial patterns were affected by the climatic zones, especially in Zone 5, as shown in Figure 4. All these cities are along the coast and impacted by the land and sea breeze. Another obvious phenomenon is that almost all the SUHIIs were clearly by the Qinling-Huaihe Line, although in Zones 1–4, the clusters were not so clearly consistent as those in Zone 5. We conclude that the spatial patterns of SUHIIs across China coincide closely with the geographical dividing line (Qinling-Huaihe Line) between North and South China (Figures 1 and 4a,b), with Zones 1 and 2 located in North China, and Zones 3–5 in South China.

As mentioned above, row normalization reduces the effects of SUHII magnitude and emphasizes similarities in temporal SUHII regimes. The SOM result obtained using row normalization in this research showed quite a complex pattern (Figure 5c). This was no surprise, as the temporal variation in the SUHII in one city was much more related to the development of urbanization [34]. The cities in each cluster are listed in Table 3. We deduced that the temporal variation patterns in the SUHIIs were related to the development of urbanization, but not the background climatic backgrounds of the cities.

Table 3. Cities in each cluster using self-organizing map (SOM) with row normalization.

Cluster	Cities
1	Shanghai, Lanzhou, Shijiazhuang, Beijing, Urumqi
2	Kunming, Guiyang, Zhengzhou, Tianjin, Laksa
3	Shenzhen, Hangzhou, Taiyuan
4	Xi'an
5	Guangzhou, Nanchang, Nanjing, Hohhot
6	Nanning, Yinchuan
7	Changsha, Wuhan, Chengdu, Jinan, Haikou
8	Fuzhou, Chongqing, Hefei, Xining, Shenyang, Changchun, Harbin

3.3. Multi-Perspective Analysis of the SUHIIs Patterns

The obvious patterns indicated in the SOM method using column and global normalization could be due to the physical geographical and radiative differences between North and South China playing the dominant role in generating the significant spatial differences in SUHI, even though intensive human activity may impact the regularity. Although obtaining direct quantitative parameters to demonstrate this effect is difficult, the much more complex spatial patterns of the daytime SUHIIs were helpful for this argument. Anthropogenic activities are much more intense and complex during the day, which considerably impact the natural environment, thus further complicating SUHI [52]. Regardless, the overall spatial patterns of the daytime SUHII in summer were still powerful evidence for this argument, as shown in Figure 6, which was derived from the annually averaged daytime SUHIIs in summer from 2003 to 2013 for each city. Overall, the spatial patterns of the SUHIIs were observed along the climate zones and obviously divided by the Qinling-Huaihe Line, exhibiting different characteristics between North and South China. The spatial patterns of the nighttime SUHIIs were also helpful in providing an explanation from the opposite point of view. As shown in Figure 4, no obvious spatial patterns in daytime SUHI in spring, summer, and autumn were observed, whereas relatively clear patterns were observed during the night. Overall, the nighttime SUHIIs in Zones 1 and 2 (North China) were significantly stronger than that in Zones 3–5 (South China).

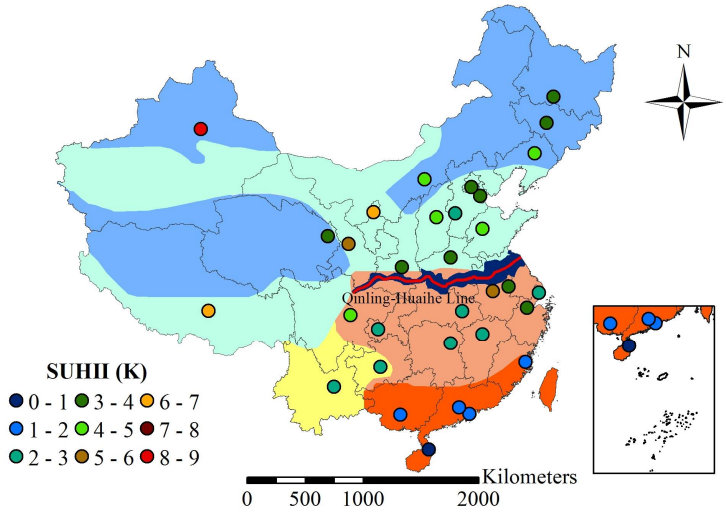

Figure 6. Spatial patterns of annual averaged daytime SUHII in summer during 2003–2013.

For the temporal regimes, the complex temporal patterns of the SUHIIs in China were due to the variation in the SUHIIs in one city being much more related to the development of urbanization. This can be inferred from urbanization background for each city listed in Table 1 and the change rate of the SUHIIs in each selected city calculated using Equation (2) in Section 2.2.2. According to the change rate presented in Figure 7 during the study period, only nine cities experienced worsening thermal environments, which was indicated by a slope greater than 0.05. These cities included Harbin, Shenyang, Changchun, Tianjin, Laksa, Kunming, Guiyang, Nanning, and Wuhan. The SUHIIs in the following 14 cities were improving: Beijing, Shanghai, Shenzhen, Guangzhou, Hangzhou, Urumqi, and Hohhot. Notably, in the first-tier mega-cities in China (Beijing, Guangzhou, and Shenzhen), the change slope of SUHII was less than -0.1, which indicates an obvious improving trend. This may be due to the urban environments in these developed cities attracting more attention and these cities are working toward being more livable cities. Conversely, the cities where the SUHIs are worsening were mostly developing cities. Regardless, the results indicated that not all the cities were experiencing worsening urban thermal environments with the development of urbanization as reported by previous studies. The urban thermal environments can be effectively improved by urban planning.

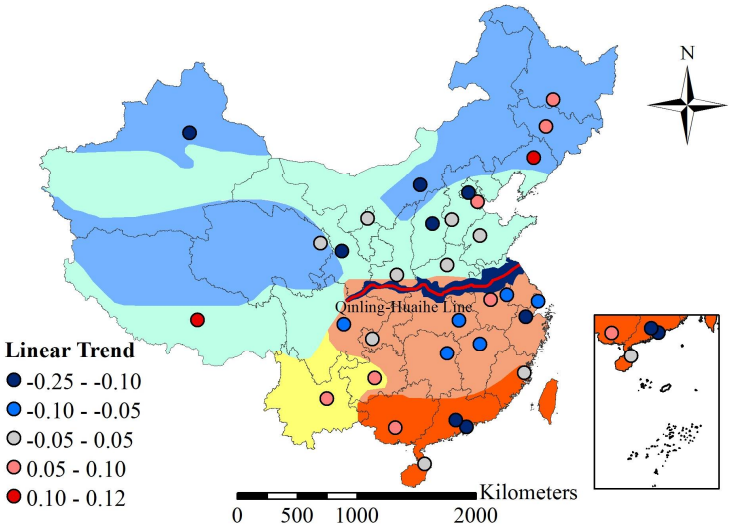

Figure 7. The change rate, or the linear trend of the seasonal averaged daytime SUHIIs, in summer from 2003 to 2013.

The SUHIIs were rather complex and comprehensively affected by various factors. Although we identified the dominant factors affecting the clusters in the spatiotemporal patterns derived from the SOM method with different normalization methods, the inherent explanation for different regions and clusters requires further study. The SOM method with the covariates and GeoDetector [53] could play an important role here.

4. Conclusions

In this research, we proposed a powerful spatiotemporal framework to study the SUHII patterns and their relationships. The results provided a regional understanding of the SUHIIs in China. We assessed the spatiotemporal variation of SUHIIs across 32 major cities in China by combining the time-series MODIS LST datasets and the LULC datasets. The SOM method was also used to reveal spatiotemporal patterns and their relationships within the selected cities in this study area. This research highlights that the significantly different processes and spatiotemporal patterns of the SUHIIs between North and South China are affected by the climatic types, especially for the background values of the SUHIIs. Moreover, the temporal variation trends in the SUHIIs in a city were mainly affected by the development of urbanization in the city.

Significant differences were observed between daytime and nighttime SUHII and between North and South China. Whereas daytime SUHIIs exhibited obvious seasonal variations across China, with the highest in summer and lowest in winter, the variations of SUHIIs in North China were comparatively much higher. Nighttime SUHIIs were much weaker and exhibited much lower seasonal variation than daytime SUHIIs, with a standard error of less than 0.3 K over the four seasons. However, nighttime SUHIIs exhibited much more obvious spatial patterns, with much higher values in North China than in South China. The physical geographical and radioactive differences between North and South China may play a dominant role in generating the significant spatial differences in SUHI. Further research is recommended in order to focus on obtaining direct quantitative parameters for examination of this finding.

In this study, another finding using the SOM method was that the SUHII in one city was much more related to its urbanization, even though the background value of the SUHII in one city was still affected by the location of the city. The urban thermal environments have effectively improved in the first-tier mega-cities in China, whereas the cities where the SUHIIs were worsening were mostly developing cities, which may be due to the focus on industrial development with little or no regard for the environment. This may be due to the fact that the urban thermal environments in those developed cities were attracting more attention and these cities have taken some measures such as green projects. Future research is also suggested to reveal the mechanisms. In any case, the results indicated that not all the cities are experiencing worsening urban thermal environments with urbanization as reported by previous studies. Urban thermal environments can be effectively improved by urban planning.

Author Contributions: J.W. designed and implemented the data analysis methods and wrote the manuscript. T.P. and C.X. supervised the data analysis, edited the manuscript. B.M. and D.F. assisted with the data analysis and manuscript preparation.

Acknowledgments: This work was supported by National Key R&D Program of China (2017YFB0503605), National Science Foundation of China (41601460), Beijing Social Science Foundation (16JDGLC014), Premium Funding Project for Academic Human Resources Development in Beijing Union University (BPHR2017DZ02), and "New Start" Academic Research Projects of Beijing Union University (ZK10201608).

Conflicts of Interest: The authors declare no conflicts of interest.

References

1. Grimm, N.B.; Faeth, S.H.; Golubiewski, N.E.; Redman, C.L.; Wu, J.G.; Bai, X.M.; Briggs, J.M. Global change and the ecology of cities. *Science* **2008**, *319*, 756–760. [CrossRef] [PubMed]
2. Oke, T.R. The energetic basis of the urban heat island. *Q. J. R. Meteorol. Soc.* **1982**, *108*, 1–24. [CrossRef]
3. Oke, T.R. City size and the urban heat island. *Atmos. Environ.* **1973**, *7*, 769–779. [CrossRef]

4. Santamouris, M.; Papanikolaou, N.; Livada, I.; Koronakis, I.; Georgakis, C.; Argiriou, A.; Assimakopoulos, D.N. On the impact of urban climate on the energy consumption of buildings. *Sol. Energy* **2001**, *70*, 201–216. [CrossRef]
5. Sarrat, C.; Lemonsu, A.; Masson, V.; Guedalia, D. Impact of urban heat island on regional atmospheric pollution. *Atmos. Environ.* **2006**, *40*, 1743–1758. [CrossRef]
6. Epstein, P.R. Climate change and human health. *N. Engl. J. Med.* **2005**, *353*, 1433–1436. [CrossRef] [PubMed]
7. Voogt, J.A.; Oke, T.R. Thermal remote sensing of urban climates. *Remote Sens. Environ.* **2003**, *86*, 370–384. [CrossRef]
8. Wang, W.C.; Zeng, Z.; Karl, T.R. Urban heat islands in China. *Geophys. Res. Lett.* **1990**, *17*, 2377–2380. [CrossRef]
9. Huang, L.; Li, J.; Zhao, D.; Zhu, J. A fieldwork study on the diurnal changes of urban microclimate in four types of ground cover and urban heat island of Nanjing, China. *Build. Environ.* **2008**, *43*, 7–17. [CrossRef]
10. Li, Q.; Zhang, H.; Liu, X.; Huang, J. Urban heat island effect on annual mean temperature during the last 50 years in China. *Theor. Appl. Climatol.* **2004**, *79*, 165–174. [CrossRef]
11. Weng, Q.H. Thermal infrared remote sensing for urban climate and environmental studies: Methods, applications, and trends. *J. Photogramm. Remote Sens.* **2009**, *64*, 335–344. [CrossRef]
12. Xiao, R.B.; Weng, Q.H.; Ouyang, Z.Y.; Li, W.F.; Schienke, E.W.; Zhang, Z.M. Land surface temperature variation and major factors in Beijing, China. *Photogramm. Eng. Remote Sens.* **2008**, *74*, 451–461. [CrossRef]
13. Li, S.S.; Gong, H.L.; Zhao, W.J.; Sun, Y.H. Analysis and study of urban heat environment and respirable particulate matter in Beijing city. *Jt. Urban Remote Sens. Event* **2009**, *1–3*, 577–582.
14. Weng, Q.H.; Lu, D.S.; Schubring, J. Estimation of land surface temperature-vegetation abundance relationship for urban heat island studies. *Remote Sens. Environ.* **2004**, *89*, 467–483. [CrossRef]
15. Shen, H.; Huang, L.; Zhang, L.; Wu, P.; Zeng, C. Long-term and fine-scale satellite monitoring of the urban heat island effect by the fusion of multi-temporal and multi-sensor remote sensed data: A 26-year case study of the city of Wuhan in China. *Remote Sens. Environ.* **2016**, *172*, 109–125. [CrossRef]
16. Fu, P.; Weng, Q. A time series analysis of urbanization induced land use and land cover change and its impact on land surface temperature with landsat imagery. *Remote Sens. Environ.* **2016**, *175*, 205–214. [CrossRef]
17. Dai, Z.; Guldmann, J.-M.; Hu, Y. Spatial regression models of park and land-use impacts on the urban heat island in central Beijing. *Sci. Total Environ.* **2018**, *626*, 1136–1147. [CrossRef]
18. Zhang, L.; Meng, Q.; Sun, Z.; Sun, Y. Spatial and temporal analysis of the mitigating effects of industrial relocation on the surface urban heat island over China. *ISPRS Int. J. Geo-Inf.* **2017**, *6*, 121. [CrossRef]
19. Buyantuyev, A.; Wu, J. Urban heat islands and landscape heterogeneity: Linking spatiotemporal variations in surface temperatures to land-cover and socioeconomic patterns. *Landsc. Ecol.* **2010**, *25*, 17–33. [CrossRef]
20. Zhou, D.; Bonafoni, S.; Zhang, L.; Wang, R. Remote sensing of the urban heat island effect in a highly populated urban agglomeration area in east China. *Sci. Total Environ.* **2018**, *628–629*, 415–429. [CrossRef] [PubMed]
21. Tran, H.; Uchihama, D.; Ochi, S.; Yasuoka, Y. Assessment with satellite data of the urban heat island effects in asian mega cities. *Int. J. Appl. Earth Obs. Geoinf.* **2006**, *8*, 34–48. [CrossRef]
22. Imhoff, M.L.; Zhang, P.; Wolfe, R.E.; Bounoua, L. Remote sensing of the urban heat island effect across biomes in the continental USA. *Remote Sens. Environ.* **2010**, *114*, 504–513. [CrossRef]
23. Pongrácz, R.; Bartholy, J.; Dezső, Z. Application of remotely sensed thermal information to urban climatology of central European cities. *Phys. Chem. Earth* **2010**, *35*, 95–99. [CrossRef]
24. Peng, S.; Piao, S.; Ciais, P.; Friedlingstein, P.; Ottle, C.; Bréon, F.-M.; Nan, H.; Zhou, L.; Myneni, R.B. Surface urban heat island across 419 global big cities. *Environ. Sci. Technol.* **2011**, *46*, 696–703. [CrossRef] [PubMed]
25. Clinton, N.; Gong, P. Modis detected surface urban heat islands and sinks: Global locations and controls. *Remote Sens. Environ.* **2013**, *134*, 294–304. [CrossRef]
26. Stewart, I.D.; Oke, T.R. Local climate zones for urban temperature studies. *Bull. Am. Meteorol. Soc.* **2012**, *93*, 1879–1900. [CrossRef]
27. Wang, K.; Wang, J.; Wang, P.; Sparrow, M.; Yang, J.; Chen, H. Influences of urbanization on surface characteristics as derived from the moderate-resolution imaging spectroradiometer: A case study for the Beijing metropolitan area. *J. Geophys. Res. Atmos.* **2007**, *112*. [CrossRef]
28. Zhang, H.; Qi, Z.; Ye, X.; Cai, Y.; Ma, W.; Chen, M. Analysis of land use/land cover change, population shift, and their effects on spatiotemporal patterns of urban heat islands in metropolitan Shanghai, China. *Appl. Geogr.* **2013**, *44*, 121–133. [CrossRef]
29. Chen, Z.; Gong, C.; Wu, J.; Yu, S. The influence of socioeconomic and topographic factors on nocturnal urban heat islands: A case study in Shenzhen, China. *Int. J. Remote Sens.* **2012**, *33*, 3834–3849. [CrossRef]

30. Chen, X.; Su, Y.; Li, D.; Huang, G.; Chen, W.; Chen, S. Study on the cooling effects of urban parks on surrounding environments using landsat tm data: A case study in Guangzhou, southern China. *Int. J. Remote Sens.* **2012**, *33*, 5889–5914. [CrossRef]
31. Zhou, X.; Wang, Y. Dynamics of land surface temperature in response to land-use/cover change. *Geogr. Res.* **2011**, *49*, 23–36. [CrossRef]
32. Xiao, H.; Weng, Q. The impact of land use and land cover changes on land surface temperature in a karst area of China. *J. Environ. Manag.* **2007**, *85*, 245–257. [CrossRef] [PubMed]
33. Bao, T.; Li, X.; Zhang, J.; Zhang, Y.; Tian, S. Assessing the distribution of urban green spaces and its anisotropic cooling distance on urban heat island pattern in Baotou, China. *ISPRS Int. J. Geo-Inf.* **2016**, *5*, 12. [CrossRef]
34. Zhou, D.; Zhang, L.; Hao, L.; Sun, G.; Liu, Y.; Zhu, C. Spatiotemporal trends of urban heat island effect along the urban development intensity gradient in China. *Sci. Total Environ.* **2016**, *544*, 617–626. [CrossRef] [PubMed]
35. Zhou, D.; Zhao, S.; Liu, S.; Zhang, L.; Zhu, C. Surface urban heat island in China's 32 major cities: Spatial patterns and drivers. *Remote Sens. Environ.* **2014**, *152*, 51–61. [CrossRef]
36. Zhou, D.; Zhao, S.; Zhang, L.; Sun, G.; Liu, Y. The footprint of urban heat island effect in China. *Sci. Rep.* **2015**, *5*, 11160. [CrossRef] [PubMed]
37. Yao, R.; Wang, L.; Huang, X.; Niu, Z.; Liu, F.; Wang, Q. Temporal trends of surface urban heat islands and associated determinants in major chinese cities. *Sci. Total Environ.* **2017**, *609*, 742–754. [CrossRef] [PubMed]
38. Kolovos, A.; Skupin, A.; Jerrett, M.; Christakos, G. Multi-perspective analysis and spatiotemporal mapping of air pollution monitoring data. *Environ. Sci. Technol.* **2010**, *44*, 6738–6744. [CrossRef] [PubMed]
39. Kohonen, T. *Self-Organizing Maps*; Springer: Berlin, Germany, 2001.
40. Delgado, T.R.; Wang, S.; Zhong, E.; Cai, W.; Long, L. Competitive learning approach to GIS based land use suitability analysis. *J. Resour. Ecol.* **2016**, *7*, 430–438. [CrossRef]
41. Agarwal, P. *Self-Organising Maps: Applications in Geographic Information Science*; John Wiley & Sons: Chichester, UK, 2008.
42. Hong, T. A close look at the China design standard for energy efficiency of public buildings. *Energy Build.* **2009**, *41*, 426–435. [CrossRef]
43. Zheng, D. *Eco-Geographical Regions in China*; Commercial Press: Beijing, China, 2008; pp. 1–387.
44. Öke, K. *The Armenian Question*; Turkish Historical Society Printing House: Ankara, Turkey, 2001; 297p.
45. Wang, J.; Huang, B.; Fu, D.; Atkinson, P. Spatiotemporal variation in surface urban heat island intensity and associated determinants across major chinese cities. *Remote Sens.* **2015**, *7*, 3670–3689. [CrossRef]
46. Bounoua, L.; Safia, A.; Masek, J.; Peters-Lidard, C.; Imhoff, M.L. Impact of urban growth on surface climate: A case study in Oran, Algeria. *J. Appl. Meteorol. Clim.* **2009**, *48*, 217–231. [CrossRef]
47. Xu, X.; Zhou, Y.X. *Urban Geography*; Higher Education Press: Beijing, China, 2008. (In Chinese)
48. Friedl, M.A.; Sulla-Menashe, D.; Tan, B.; Schneider, A.; Ramankutty, N.; Sibley, A.; Huang, X. Modis collection 5 global land cover: Algorithm refinements and characterization of new datasets. *Remote Sens. Environ.* **2010**, *114*, 168–182. [CrossRef]
49. Heyden, Y.V.; Vankeerberghen, P.; Novic, M.; Zupan, J.; Massart, D.L. The application of Kohonen neural networks to diagnose calibration problems in atomic absorption spectrometry. *Talanta* **2000**, *51*, 455–466. [CrossRef]
50. Carnahan, W.H.; Larson, R.C. An analysis of an urban heat sink. *Remote Sens. Environ.* **1990**, *33*, 65–71. [CrossRef]
51. Schwarz, N.; Schlink, U.; Franck, U.; Großmann, K. Relationship of land surface and air temperatures and its implications for quantifying urban heat island indicators: An application for the city of Leipzig (Germany). *Ecol. Indic.* **2012**, *18*, 693–704. [CrossRef]
52. Sailor, D.J.; Lu, L. A top-down methodology for developing diurnal and seasonal anthropogenic heating profiles for urban areas. *Atmos. Environ.* **2004**, *38*, 2737–2748. [CrossRef]
53. Wang, J.F.; Li, X.H.; Christakos, G.; Liao, Y.L.; Zhang, T.; Gu, X.; Zheng, X.Y. Geographical detectors-based health risk assessment and its application in the neural tube defects study of the Heshun region, China. *Int. J. Geogr. Inf. Sci.* **2010**, *24*, 107–127. [CrossRef]